The boron-oxygen (B_iO_i) defect complex induced by irradiation with 6 MeV electrons in p-type silicon diodes

Chuan Liao[a], E. Fretwurst[a], E. Garutti[a], J.Schwandt[a]

[a]Institut für Experimentalphysik, Universität Hamburg

A. Himmerlich[b], Y. Gurimskaya[b], I. Mateu[b], M. Moll[b]

[b]Conseil européen pour la recherche nucléaire (CERN)

I. Pintilie[c]

[c]National Institute of Materials Physics (NIMP)

L. Makarenko[d]

[d]Belarussian State University

RD50

June 21, 2021

Outline

I. Motivation

II. Experimental details

III. Measurement results for as-irradiated

IV. Measurement results for annealing behavior

V. Summary

Motivation

Radiation damage of LGADs [1] (Low Gain Avalanche Diodes)

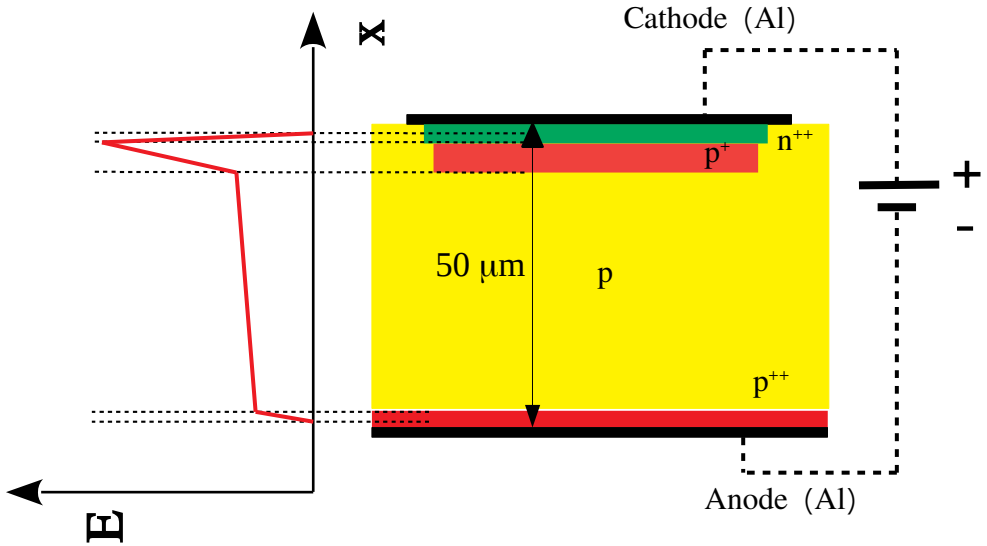

Fig. 1 Schematic of LGAD

- Aluminum
- p type bulk (Boron doping, ~10^{13} cm^{-3})
- p^+ (Boron doping B_s^-, ~ 10^{16} cm^{-3})
- p^{++} (Boron doping B_s^-, ~ 10^{19} cm^{-3})
- n^{++} (phosphorus doping P_s^+, ~ 10^{21} cm^{-3})

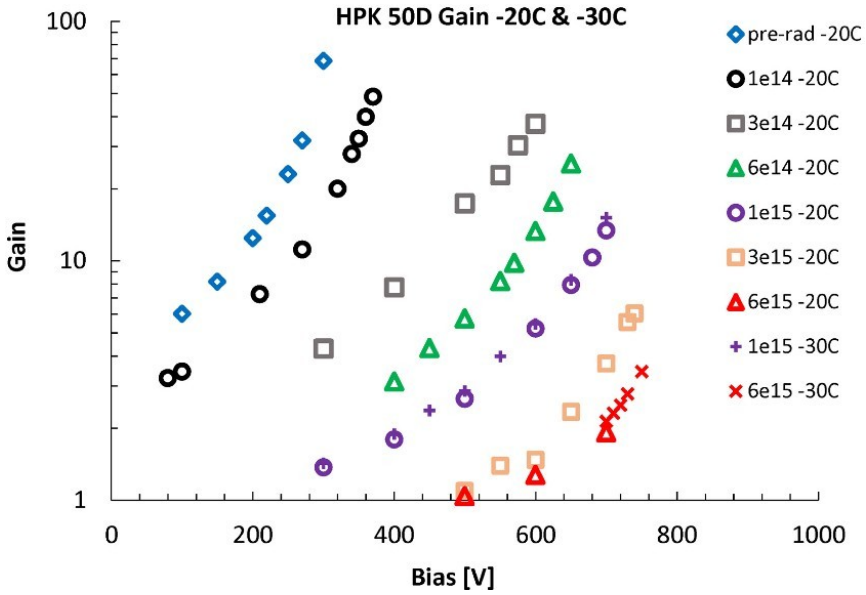

Fig. 2 Gain value vs. bias for different fluences

Significant decrease of Gain value after irradiation

[1] Kramberger, G., et al. "Radiation effects in Low Gain Avalanche Detectors after hadron irradiations." Journal of Instrumentation 10.07 (2015): P07006.

Motivation

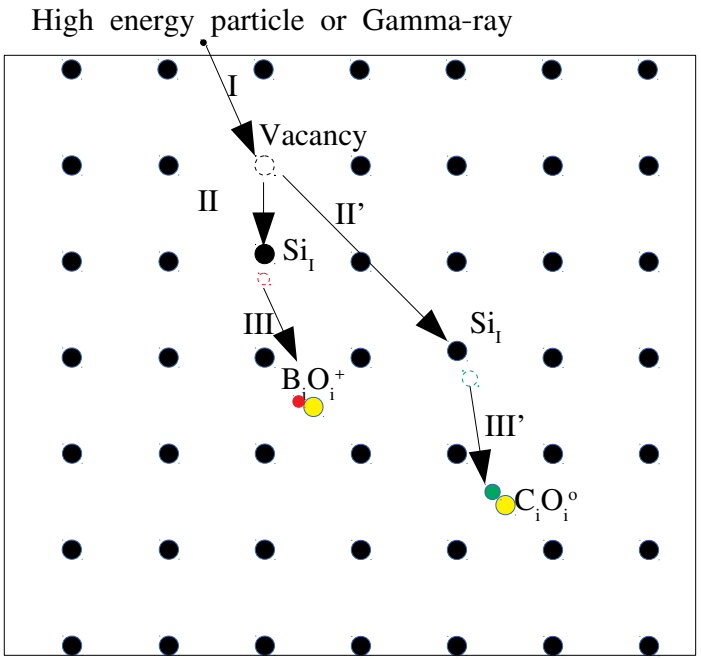

Fig.3 Schematic of radiation damage in p-type silicon material

I: Lattice Silicon atom (Si_s) was knocked out by incident particle and Si_s got recoil energy and turns to interstitial silicon (Si_i)

II: Si_i diffusion in the bulk and impact on Lattice Boron atom (B_s)

III: B_s was knocked out Si_i and turns to interstitial Boron (B_I) and finally captured by interstitial Oxygen (O_i)

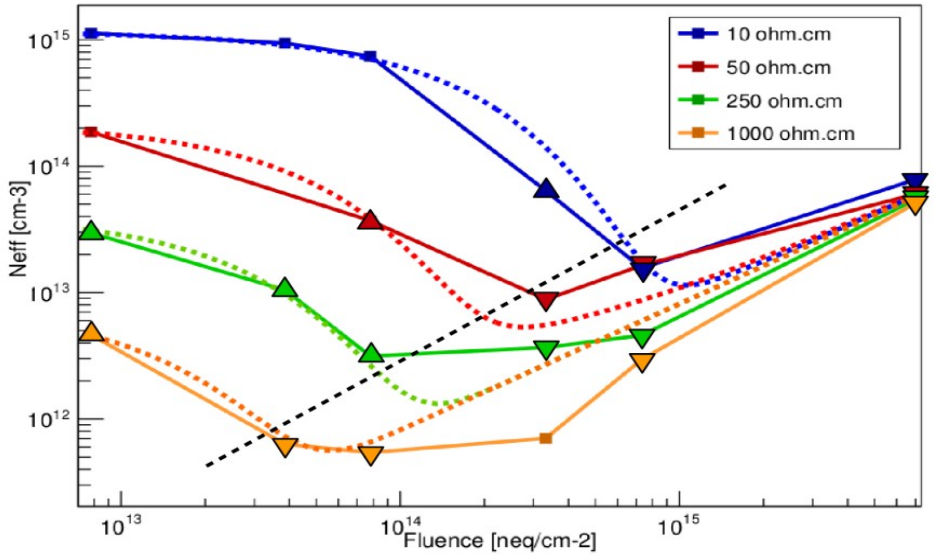

Fig. 4 N_{eff} vs. fluence for different initial doping concentration

Radiation damage of p-type diodes is dominated by acceptor removal in the beginning and afterwards by acceptor generation [1]

B^- turn to $B_iO_i^+$

Change in N_{eff} is a factor of 2 and it will significantly affect the distribution of electric field.

[1] Y. Gurimskaya, 31st RD50 Workshop, 20-22 of November, 2017, CERN, Geneva, Switzerland.

Experimental detail

Information of measured expitaxial silicon diodes

Label	EPI50P_06_DS_3	EPI50P_06_DS_5	EPI50P_06_DS_7	EPI50P_06_DS_9
$N_{eff,0}$	P-type 0.8e15 cm^{-3}			
Initial resistivity	~ 10 Ωcm			
Irradiation (6 MeV electrons)	1e15 e/cm^2 (3.98e13 n_{eq}/cm^2)	2e15 e/cm^2 (7.96e13 n_{eq}/cm^2)	4e15 e/cm^2 (1.59e14 n_{eq}/cm^2)	6e15 e/cm^2 (2.39e14 n_{eq}/cm^2)
Area	6.21E-2 cm^2			
Thickness	50 μm			

C-V, I-V:

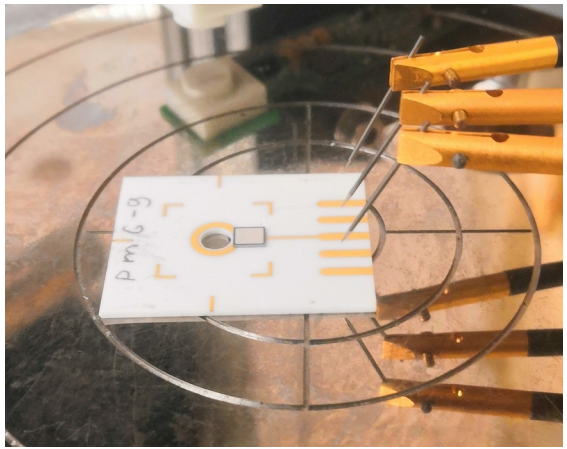

Experimental parameter (C-V, I-V):

Temperature: 20 °C
Humidity: < 10%
Frequencies for C-V: 230 Hz, 455 Hz, 1 kHz, 10 kHz
AC voltage for C-V: 0.5 V

Experimental parameter (TSC and TS-Cap):

Cooling down bias: 0 V
Filling temperature: typical 10 K
Filling: Forward bias filling, 0 V filling or light injection
Filling time: 30 s
Delay time: 30 s
Heating rate: 0.183 K/s

Thermally stimulated current and Thermally stimulated capacitance (TSC, TS-Cap):

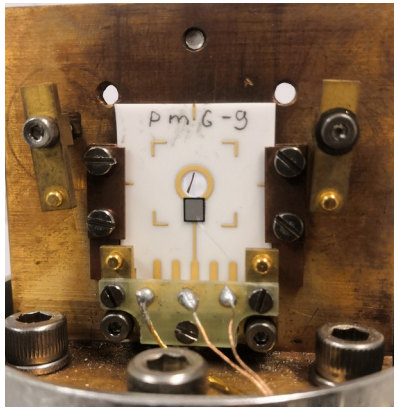

Experimental detail

Basic Principle of Thermally Stimulated Current-TSC (or TS-Cap) [2]:

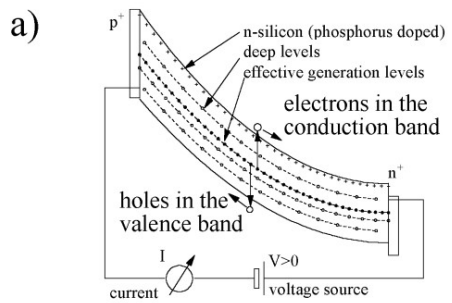

Fig. 5a Cooling

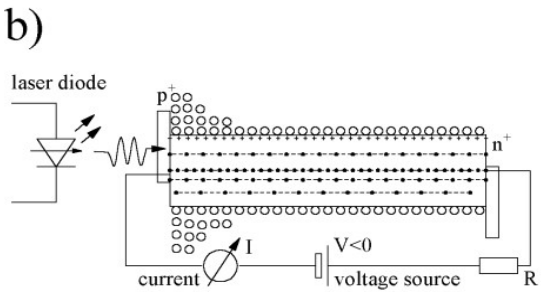

Fig. 5b Injection:
Forward bias injection, light injection and majority carriers injection.

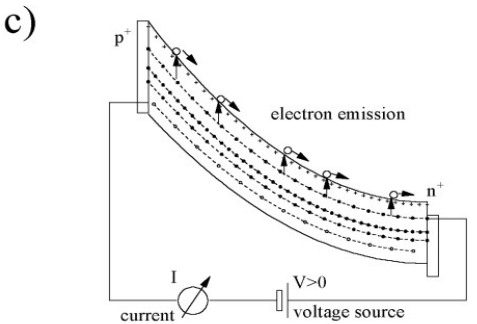

Fig. 5c Recording data

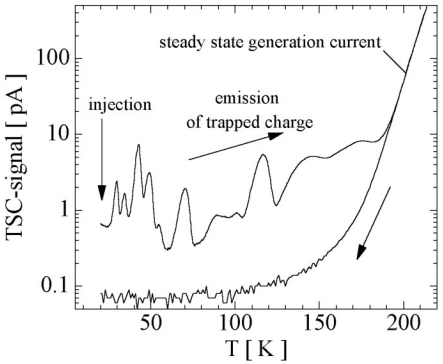

Fig. 6 TSC spectrum [2]

$$I_{tsc} = \frac{1}{2} q_0 A d N_t e_n \exp\left(-\frac{1}{\beta}\int e_n(T)dT\right)$$

$$e_n = \sigma_n \nu_{th,n} N_c \times \exp\left(\frac{-E_a}{k_B T}\right)$$

$$E_a = E_C - E_T$$

N_t is defect concentration; β is heating rate; σ_n is capture cross section; E_a is activation energy; A is diodes area; d depleted thickness; [1]

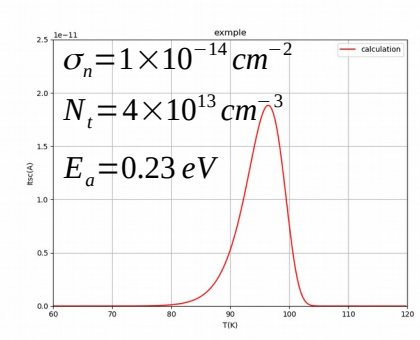

Fig.7 example of calculated TSC peak

[1] Buehler, M. G. Solid-State Electronics 15.1 (1972): 69-79.
[2] Moll, Michael. Radiation damage in silicon particle detectors: Microscopic defects and macroscopic properties. No. DESY-THESIS-1999-040. DESY, 1999.

I-V and N_{eff} profile (10 Ωcm, as-irrad)

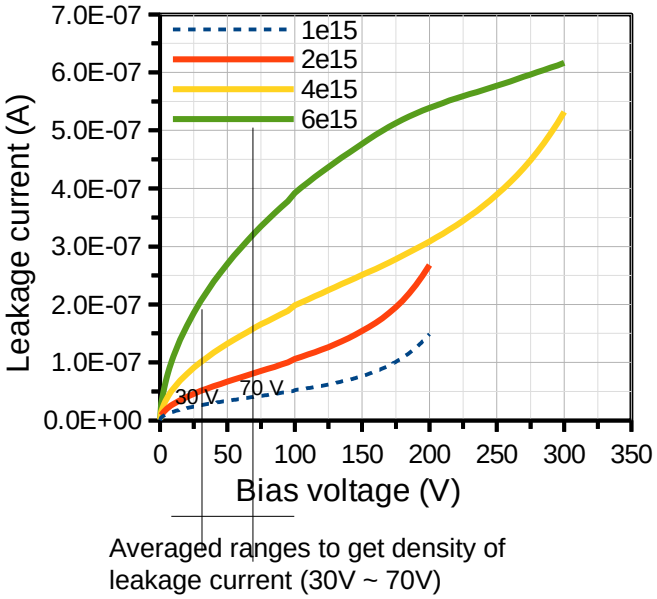

Fig. 8 Leakage current for different fluence

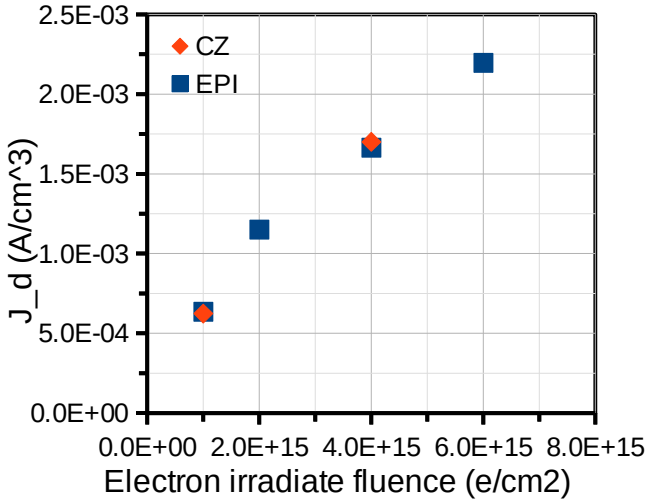

Fig. 9 Mean value of leakage current density J_d as function of irradiation fluence

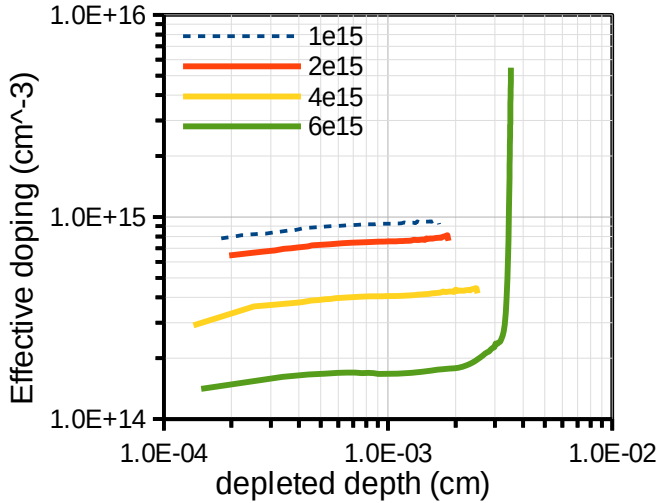

Fig. 10 Doping profile

- Leakage current increases with fluence. In order to observe the mean value of leakage current density (J_d), the current in the range from 30V to 70V was chosen for calculate J_d (the depleted volume is taken from C-V measurement)
- Doping profile is taken from C-V measurement with frequency equal 10 kHz and V_{AC}=0.5V. Effective doping decrease with fluence

Example of TSC on BiOi (10 Ωcm, as-irrad)

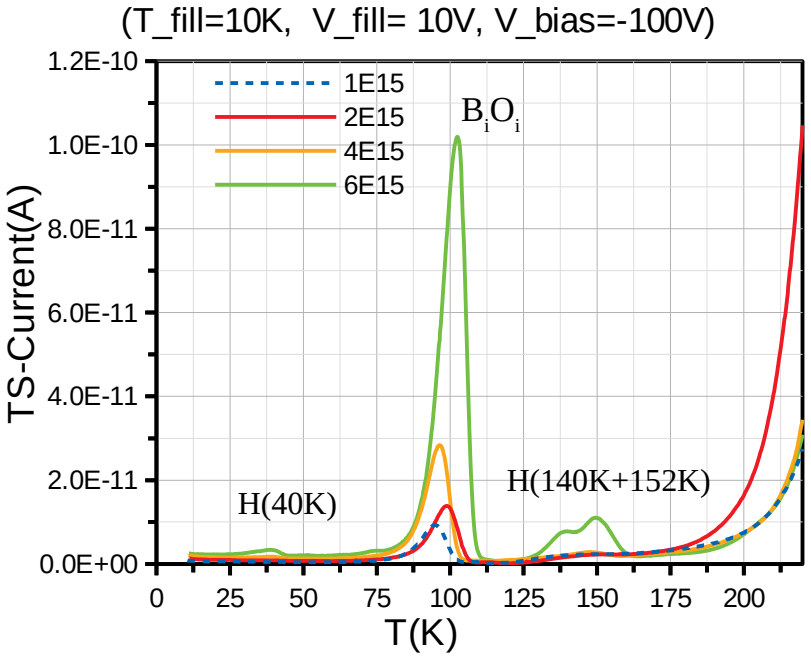

Fig. 11 TSC spectra for diodes with different irradiation fluence

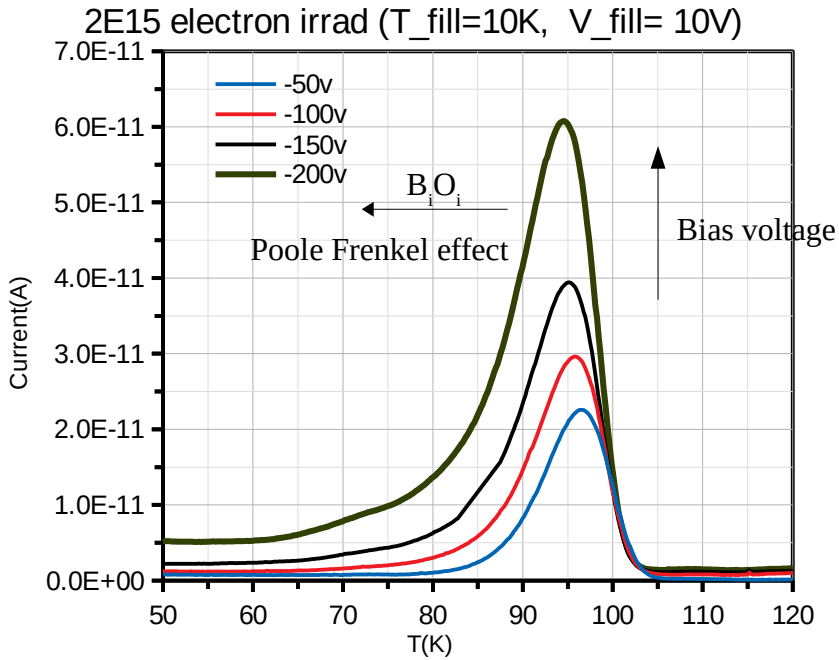

Fig. 12 TSC spectra for different reverse bias heating up

- Dominant B_iO_i signal, which depends on the fluence.
- Shift peak maximum with V_{bias} → Poole-Frenkel effect; electron trap B_iO_i (o/+) donor defect
- Peak amplitude increases with bias voltage due to increasing depletion depth

Example of TS-Cap on B_iO_i (10 Ωcm, as-irrad)

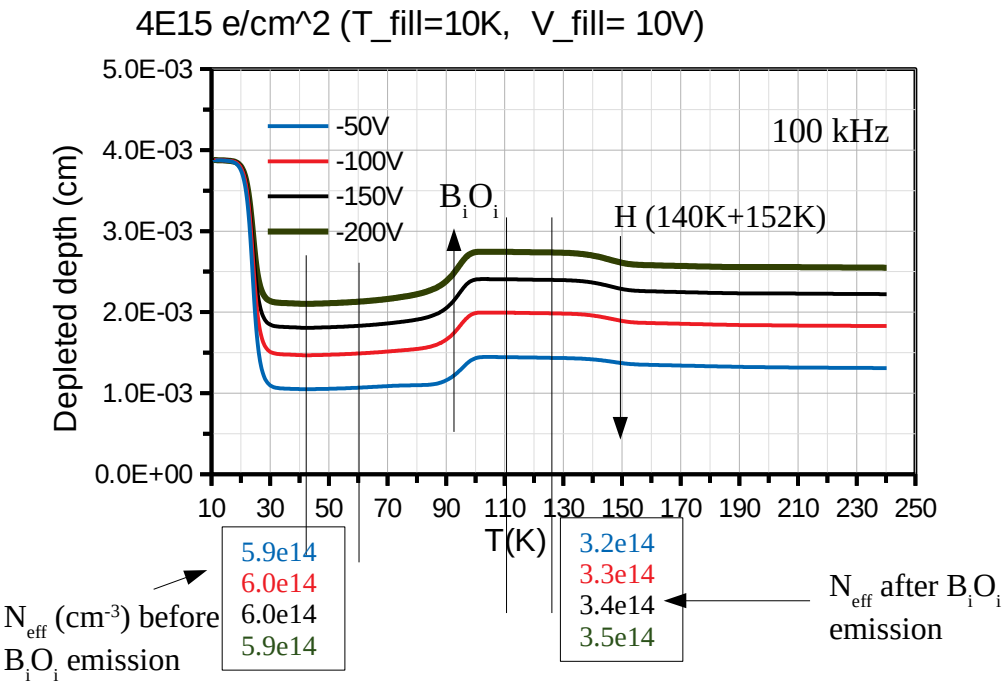

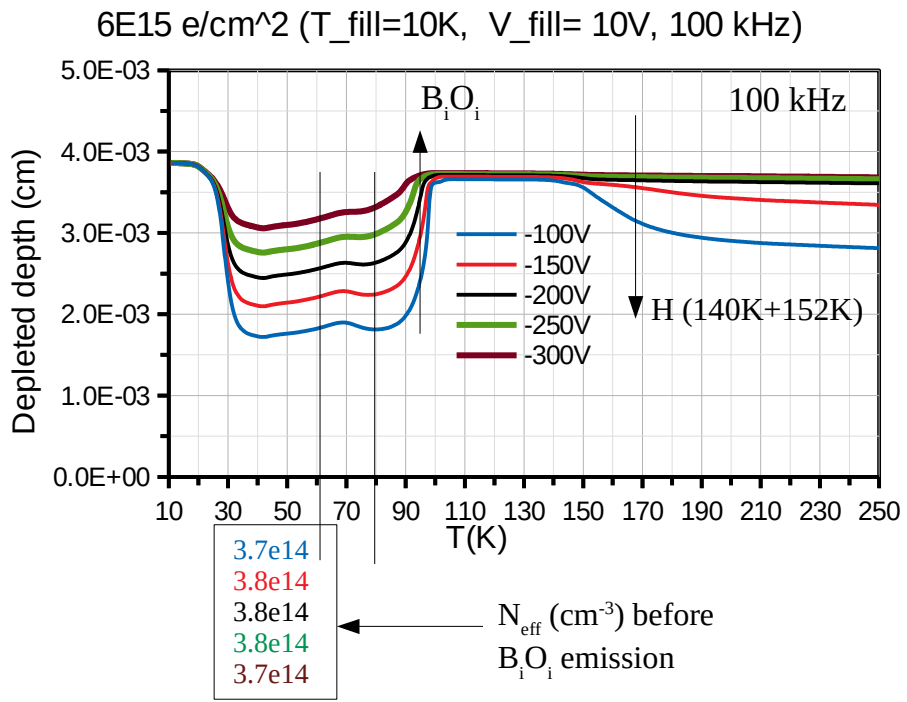

- Depleted depth was extracted from TS-cap with $d = \varepsilon_{si}\varepsilon_0 A/C$
- The shift of B_iO_i peak temperature versus V_{bias} can also be observed in TS-Cap measurement
- Freeze-out of free charge carriers for T < 40 K
- Effective doping concentration can be extracted only if the diode is not fully depleted

Defect concentration and introduction rate (as-irrad)

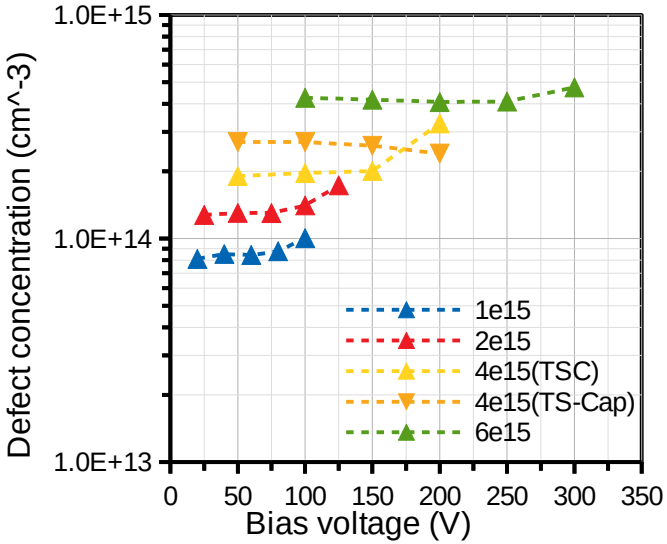

$$N_t(V) = \sum_i \frac{2Q_i}{q_0 A\, w(T_i)} (1)$$

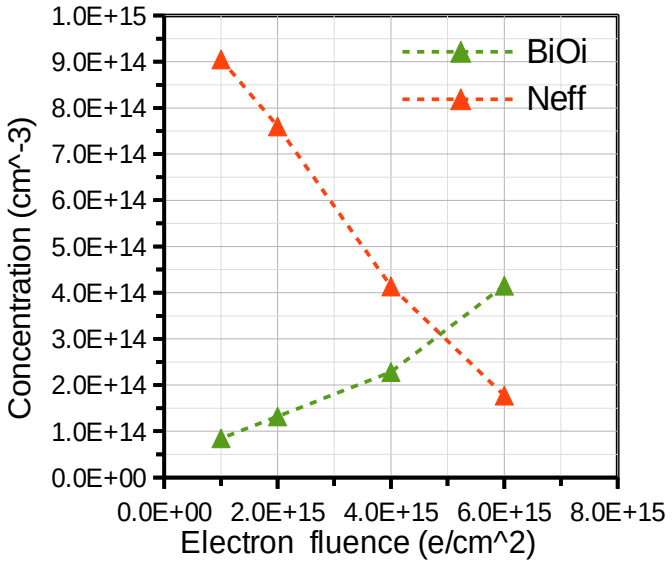

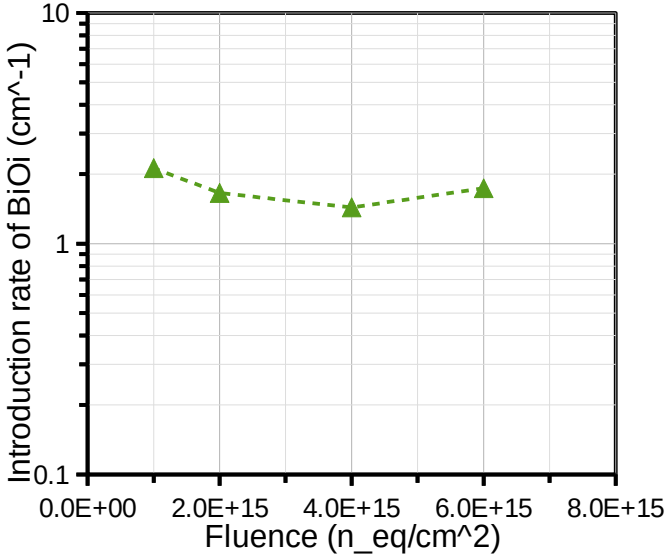

$$g(B_iO_i) = \frac{N_t(V)}{\phi_{eq}} (2)$$

- B_iO_i concentration of 1e15 diode and 2e15 diode are given by integration with constant depletion depth (w, which is given by C-V measurment) from 80 K to 110 K
- Defect concentration of 4e15 diode and 6e15 diode are given by the eq.(1) and sum from 80 K to 110 K.
- Effective doping (N_{eff}) is extracted from fig. 10 doping profile

Annealing behavior (Leakage current)

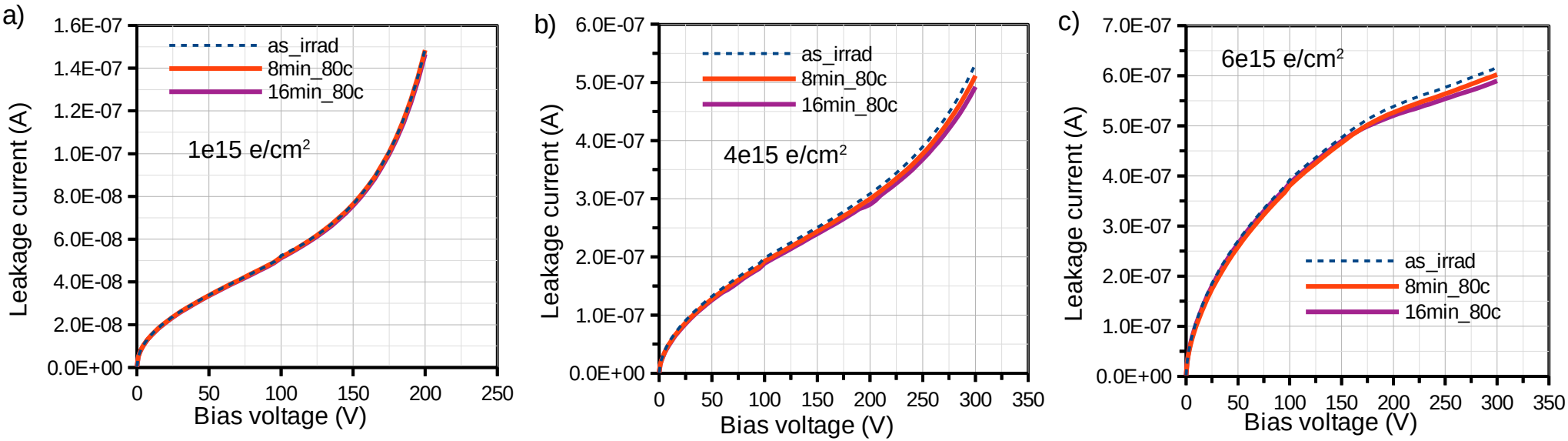

Leakage current for different annealing steps of diode irradiated by 6 MeV electron

- The leakage current slightly changes during isothermal annealing at 80 °C

Annealing behavior (doping profile)

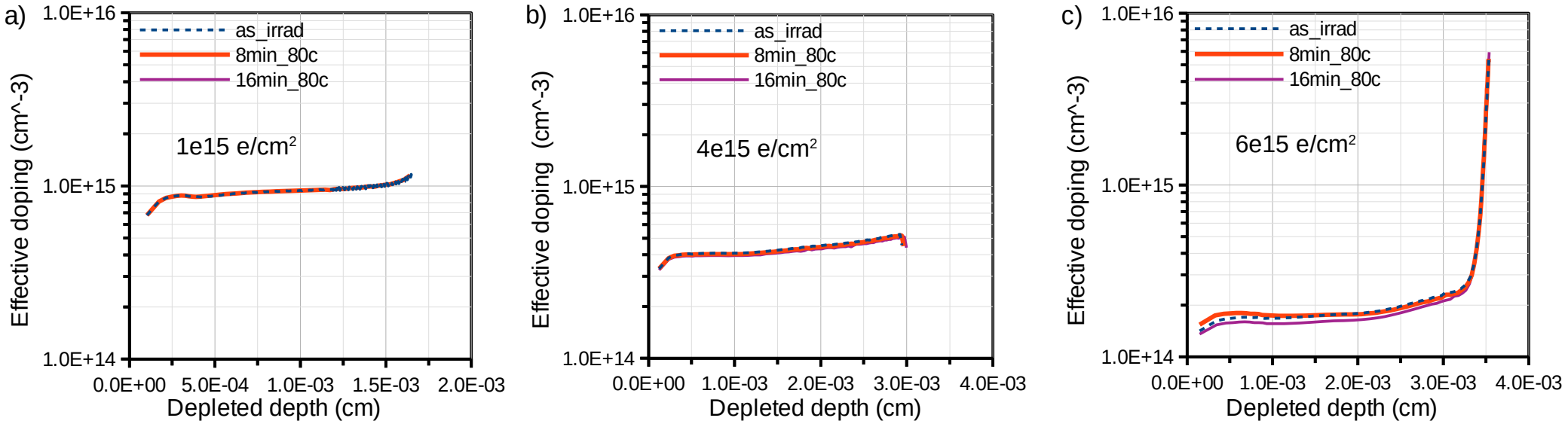

Doping profile for different annealing steps of diode irradiated by 6 MeV electron

- The doping profile slightly changes during isothermal annealing at 80 °C due to the B_iO_i is stable in the bulk

Annealing behavior (J_d and B_iO_i concentration)

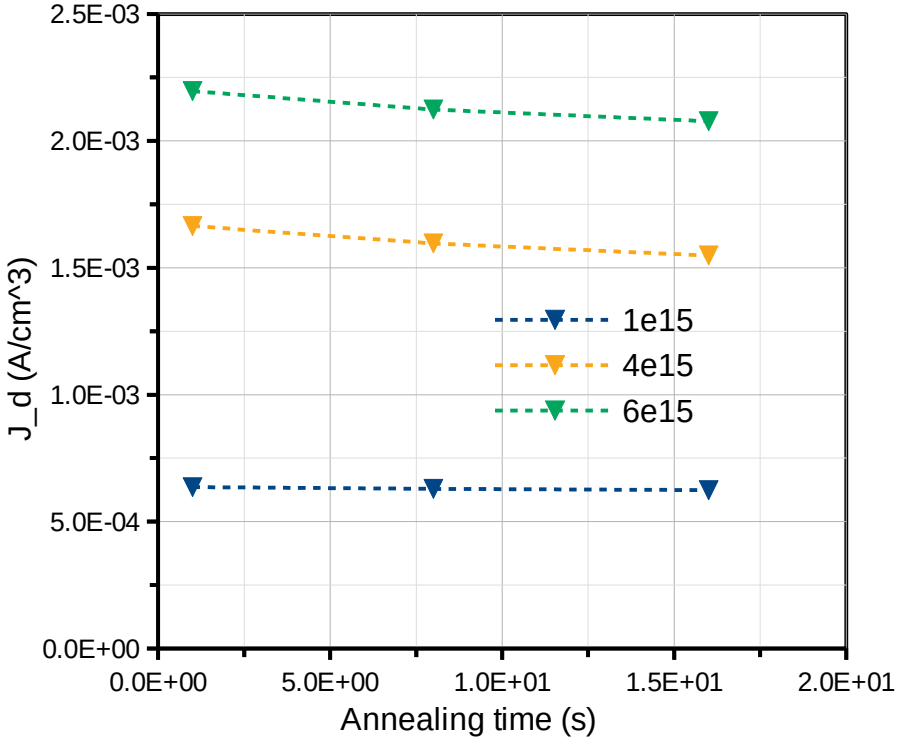

Fig. 20 Mean value of leakage current density J_d as function of annealing time

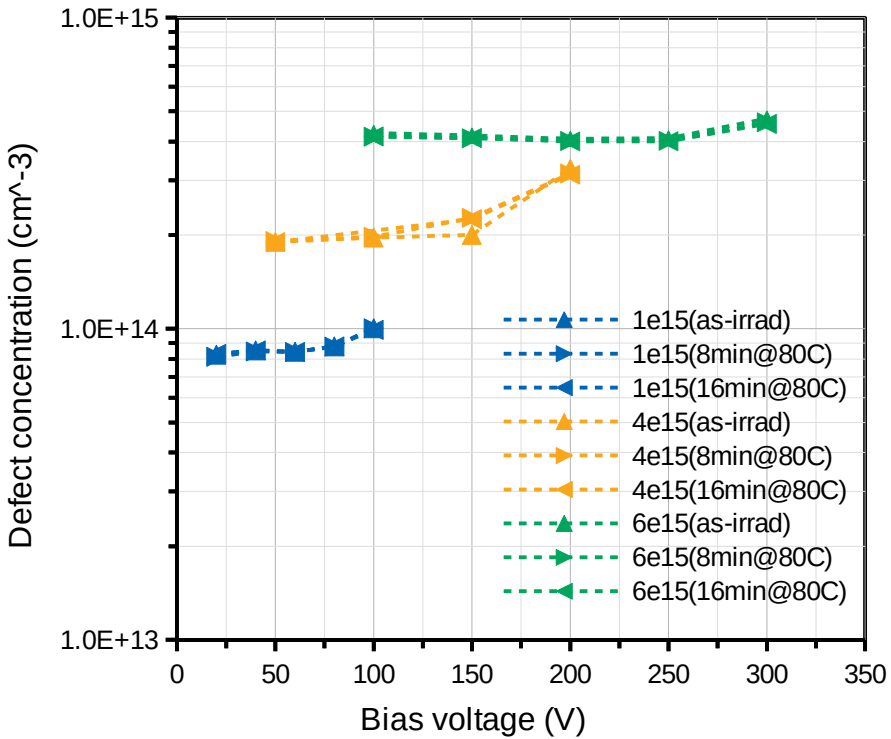

Fig. 21 BiOi concentration as function of bias for different annealing steps

- J_d and BiOi are stable during isothermal annealing at 80 °C

Summary

I. Results for ~10 Ωcm diodes irradiated by 6 MeV electron with fluence (1e15 e/cm^2, 2e15 e/cm^2, 4e15 e/cm^2 and 6e15 e/cm^2):

a). Macroscopic measurement (I-V, C-V):

- Leakage current increases and effective doping decreases as fluence increasing
- Leakage current and doping profile are stable during isothermal annealing at 80 ^{o}C

b). Microscopic measurement (TSC, TS-Cap):

- B_iO_i peak on TSC spectra: 3-D Poole Frenkel effect (shift with bias voltage)
- B_iO_i concentration proportion to irradiated fluence
- B_iO_i introduction rate (g_{BiOi}) is nearly the same for the different fluence
- The different B_iO_i concentration extracted from TSC and TS-Cap
- B_iO_i are stable during isothermal annealing at 80 ^{o}C

II. Comparison with 23 GeV proton [1]:

- Macroscopic measurement (I-V, C-V): Leakage current significantly decrease during isothermal annealing at 80 ^{o}C (Proton)
- Microscopic measurement (TSC): $2 * g_{BiOi,\ 23\ GeV\ proton} \approx g_{BiOi,\ 6\ MeV\ electron}$

Further plans :

I. Describe the TSC peak with temperature dependent depleted depth and electric field

II. Figure out the reason why the BiOi concentration shows difference between TSC and TS-Cap

III. Investigate LGADs

[1] C. Liao 37th RD50 Workshop, Nov 2020, Zagreb.

Back up

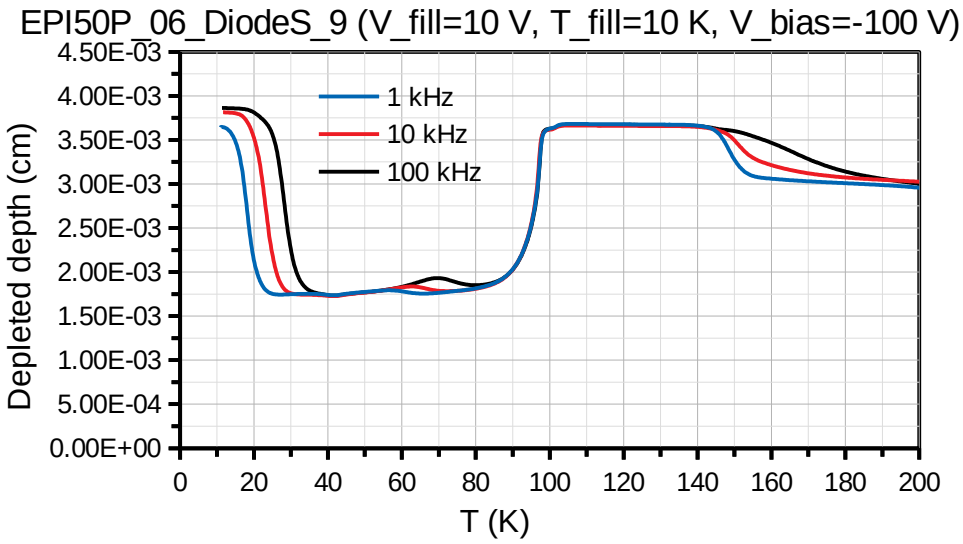
EPI50P_06_DiodeS_9 (V_fill=10 V, T_fill=10 K, V_bias=-100 V)
Depleted depth (cm)
4.50E-03
4.00E-03
3.50E-03
3.00E-03
2.50E-03
2.00E-03
1.50E-03
1.00E-03
5.00E-04
0.00E+00
0
20
40
60
80
100
120
140
160
180
200
T (K)
1 kHz
10 kHz
100 kHz

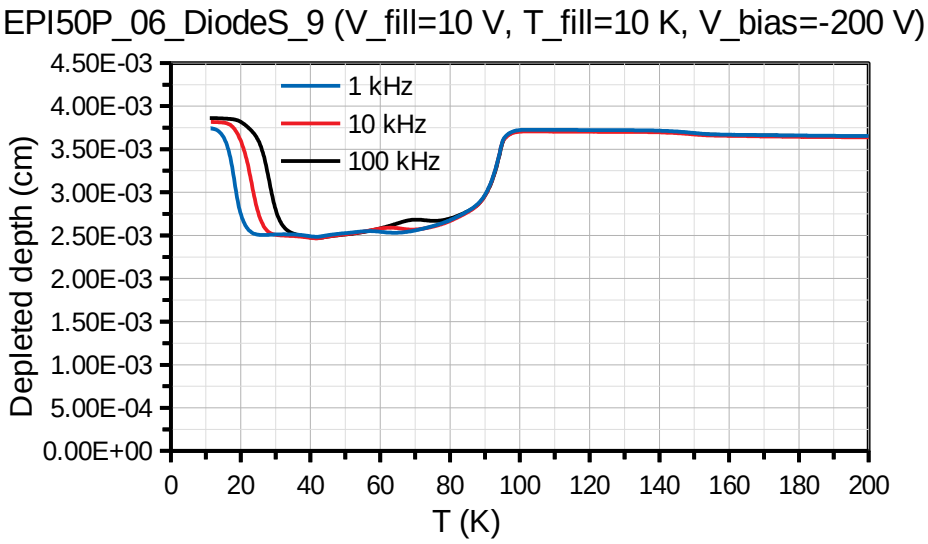
EPI50P_06_DiodeS_9 (V_fill=10 V, T_fill=10 K, V_bias=-200 V)
Depleted depth (cm)
4.50E-03
4.00E-03
3.50E-03
3.00E-03
2.50E-03
2.00E-03
1.50E-03
1.00E-03
5.00E-04
0.00E+00
0
20
40
60
80
100
120
140
160
180
200
T (K)
1 kHz
10 kHz
100 kHz

Back up

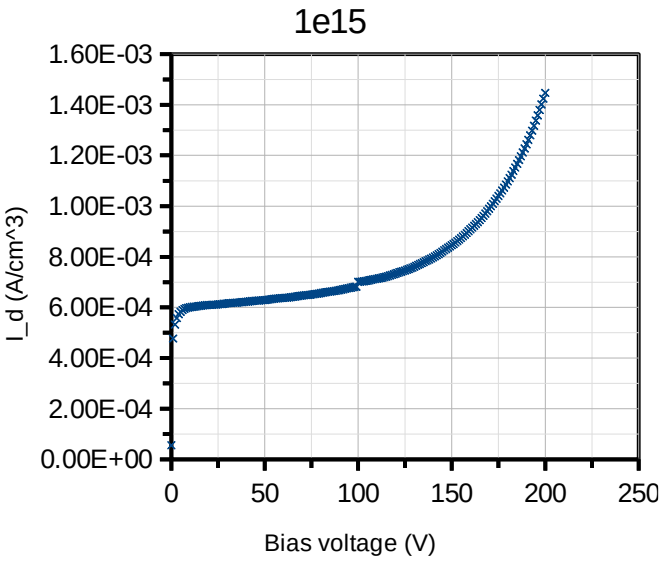
1e15
1.60E-03
1.40E-03
1.20E-03
1.00E-03
8.00E-04
6.00E-04
4.00E-04
2.00E-04
0.00E+00
I_d (A/cm^3)
0
50
100
150
200
250
Bias voltage (V)

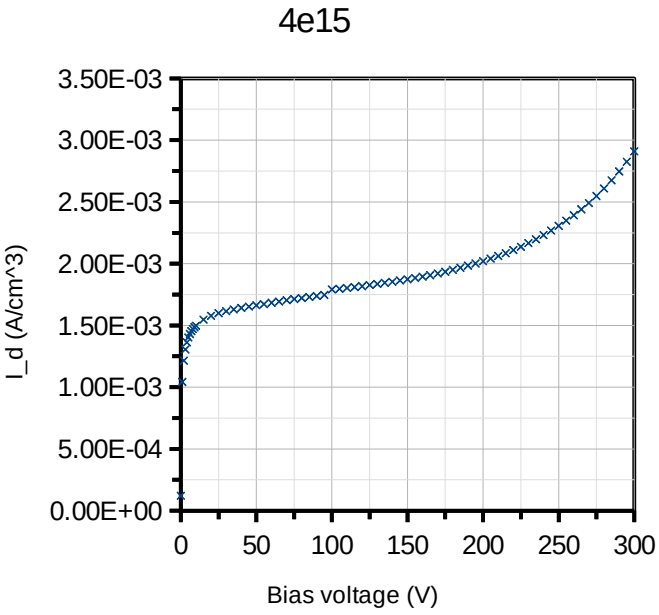
4e15
3.50E-03
3.00E-03
2.50E-03
2.00E-03
1.50E-03
1.00E-03
5.00E-04
0.00E+00
I_d (A/cm^3)
0
50
100
150
200
250
300
Bias voltage (V)

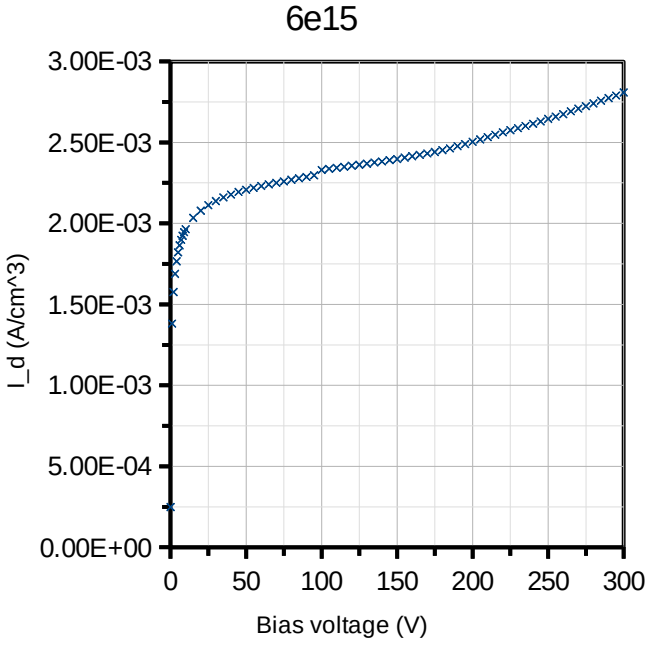
6e15
3.00E-03
2.50E-03
2.00E-03
1.50E-03
1.00E-03
5.00E-04
0.00E+00
I_d (A/cm^3)
0
50
100
150
200
250
300
Bias voltage (V)

Back up

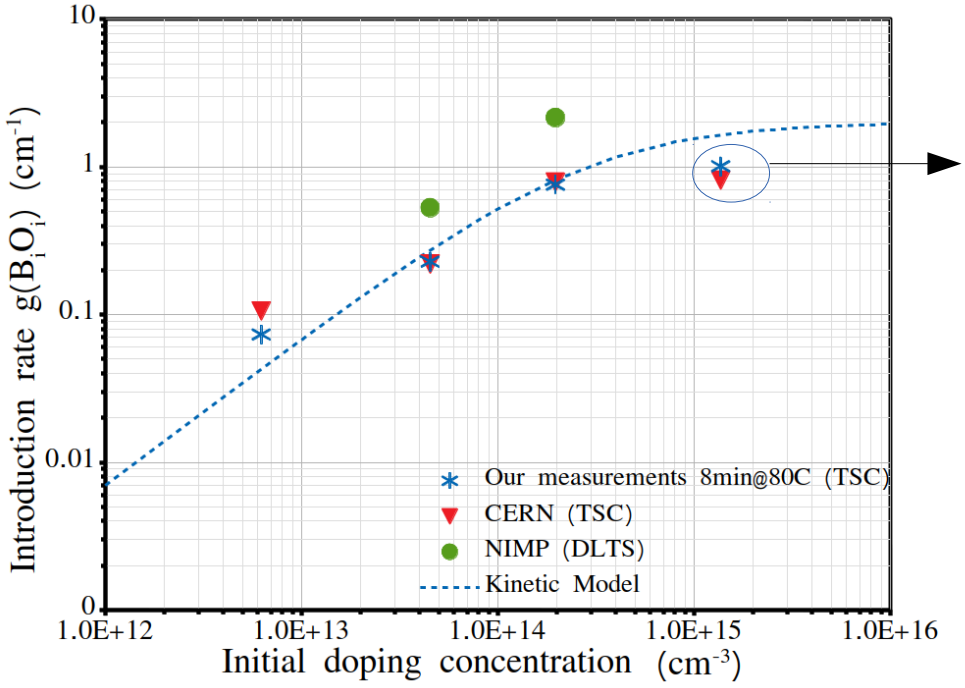

< 1 cm^{-1}, roughly 2 cm^{-1} for electron irradiated

Introduction rate of B_iO_i

(our measurement was shown in the figure is 23 GeV proton irradiated with fluence 4.28e13 n_{eq}/cm^2)

Back up

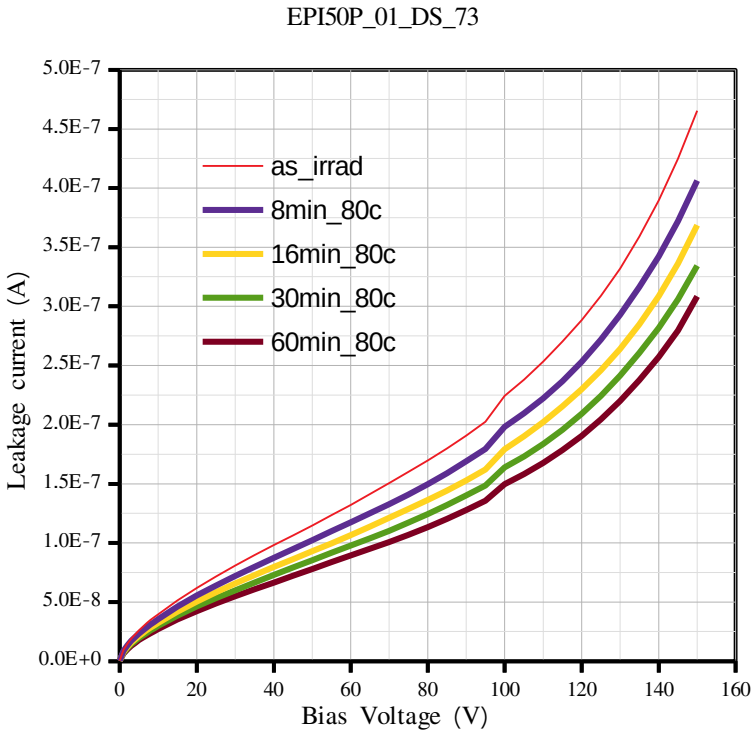

I-V measurement for diode with 1e15 effective doping and irradiated by 23GeV with fluence 4.28e13 n_{eq}/cm^2

Leakage current significantly decrease during isothermal annealing at 80 °C